



Cite this: Analyst, 2015, 140, 2383

## Comparison of transmission and transfectance mode FTIR imaging of biological tissue

Michael J. Pilling,<sup>a,b</sup> Paul Bassan<sup>a,b,c</sup> and Peter Gardner<sup>\*a,b</sup>

FTIR microscopy is a powerful technique which has become popular due to its ability to provide complementary information during histopathological assessment of biomedical tissue samples. Recently however, questions have been raised on the suitability of the transfection mode of operation for clinical diagnosis due to the so called Electric Field Standing Wave (EFSW) effect. In this paper we compare chemical images measured in transmission and transfection from prostate tissue obtained from five different patients, and discuss the variability of the spectra acquired with each sampling modality. We find that spectra obtained in transfection undergo a non-linear distortion, *i.e.* non-linear variations in absorption band strength across the spectra, and that there are significant differences in spectra measured from the same area of tissue depending on the mode of operation. Principal Component Analysis (PCA) is used to highlight that poorer discrimination between benign and cancerous tissue is obtained in transfection mode. In addition we show that use of second derivatives, while qualitatively improves spectral discrimination, does not completely alleviate the underlying problem.

Received 29th October 2014,  
Accepted 2nd February 2015

DOI: 10.1039/c4an01975j

[www.rsc.org/analyst](http://www.rsc.org/analyst)

### 1. Introduction

Infrared spectroscopic microscopy has become a highly regarded technique for investigating biological systems. The ability to obtain the high spatial resolution of optical microscopy coupled with the chemical information from vibrational spectroscopy has driven its rapid expansion within the biosciences. Over the past decade there has been increasing interest in utilising chemical imaging for the diagnosis of disease.<sup>1–8</sup> However successful implementation of infrared microscopy in the clinical environment requires a number of significant barriers to be overcome. Traditionally infrared microscopy studies of tissue have been conducted in transmission mode, where infrared light passes through a thin section of the tissue (typically 4–10 µm) on an infrared transparent material. Barium or calcium fluoride slides are commonly used as the substrate, but have the disadvantage that they are both expensive and somewhat fragile making them generally less suitable for use in a clinical laboratory. These barriers to practical application have given rise to an increase in popularity of the reflection-absorption, or so-called transfection mode of operation.<sup>9–12</sup> In transfection, the sample is

mounted on a highly reflective substrate and the infrared light is transmitted through the sample, reflects off the top layer of the substrate and then passes through the sample a second time, effectively doubling the pathlength and increasing the sensitivity. Ag/SnO<sub>2</sub> coated glass slides (often called low emissivity slides) are commonly used as transfection substrates and they have the advantage that they are cheap and robust. Recent studies however have suggested that caution needs to be exercised when utilising the transfection mode of operation, due to spectral distortions arising from the so-called Electric Field Standing Wave (EFSW) effect.<sup>13–16</sup>

The Electric Field Standing Wave effect originates from the interaction of electromagnetic radiation with a reflective surface. Infrared radiation impinging at normal incidence undergoes a phase change of approximately 180° upon reflection. The interaction of the incident and reflected rays causes the creation of a sinusoidal electric field standing wave with a node formed at the surface and an anti-node  $\frac{1}{4} \lambda$  from the surface.<sup>17</sup> In the case of a focussed beam there is a narrow spread of near normal angles of incidence, this results in an elliptical ‘standing wave’ being formed which is similar to the standing wave formed at normal incidence. Brooke<sup>18</sup> observed this effect while investigating multilayer polymer microspheres in transfection mode, and found that the absorbance band intensity did not change linearly for samples of varying thickness. It is crucially important to understand the implications of these distortions for chemical imaging of biological tissue.

In this paper we compare chemical images obtained in transmission and transfection from prostate tissue from five

<sup>a</sup>Manchester Institute of Biotechnology, University of Manchester, 131 Princess Street, Manchester, M1 7DN, UK. E-mail: Peter.Gardner@Manchester.ac.uk; Fax: +44 (0)161 306 5201; Tel: +44 (0)161 306 4463

<sup>b</sup>School of Chemical Engineering and Analytical Science, University of Manchester, Oxford Road, Manchester, M13 9PL, UK

<sup>c</sup>London Spectroscopy Ltd, 6 Lennard Road, Dunton Green, London, TN13 2UU, UK

different patients, and discuss the differences observed in each mode of operation. We investigate the variability of spectra for each of the five patients obtained within each technique through analysis of distributions of absorption band intensity, and discuss the implications for histological classification and cancer diagnosis.

## 2. Materials and methods

Formalin fixed paraffin embedded (FFPE) prostate tissue specimens were acquired following informed consent and in accordance with ethical approval (Trent Multi-centre Research Ethics Committee 01/4/061). The tissue was obtained from five separate patients, consisting of three diagnosed with benign prostatic hyperplasia (BPH), and two with prostate cancer (CaP) during a *trans*-urethral resection of the prostate (TURP). A serial section of 4 µm thickness was cut from each tissue block, mounted on a glass slide and underwent haematoxylin and eosin (H&E) histological staining for histopathological assessment. Two further contiguous serial sections were taken, the first was prepared onto a calcium fluoride substrate of 1 mm thickness for transmission infrared chemical imaging. The second section was prepared onto a low-e MirrIR slide (Kevley Technologies, Ohio, USA) for transfection mode imaging.

Tissue sections on the MirrIR and calcium fluoride slides were de-waxed following a standard local histological protocol. Each tissue sample was de-waxed by dipping ten times in a beaker containing xylene, and then allowed to rest submerged in the beaker for a duration of fifteen minutes. The process was repeated three times more with fresh xylene, and then the sample was removed and allowed to air dry at room temperature for 24 hours.<sup>19</sup>

FT-IR chemical images were collected using a Varian 670 Infrared spectrometer coupled to a Varian 620-IR imaging microscope equipped with a 128 × 128 pixel liquid nitrogen, cooled Mercury Cadmium telluride (MCT) focal plane array detector. The infrared microscope consists of a ×15 magnification objective with a resultant field of view of 704 µm. Chemical images of the tissues were acquired *via* collection of a series of infrared tiles (each 704 µm × 704 µm) which were then reconstructed post collection to form a single infrared image. Spectra were collected at 8 cm<sup>-1</sup> spectral resolution (generally deemed sufficient for good classification)<sup>2</sup> by the co-addition of 256 and 8 scans for the background and each mosaic tile respectively. The interferograms were processed using triangular apodization with 1 level of zero filling giving a data point spacing of approximately 4 cm<sup>-1</sup>, with the spectral range 900–4000 cm<sup>-1</sup> retained.

All pre-processing and data analysis was performed using Matlab 2012a (The MathWorks Inc., Natick, MA) and the Prospect Toolbox (London Spectroscopy Ltd, London, UK). Initial pre-processing included implementation of a noise reduction algorithm based on principal component analysis. Noise reduction is achieved in this method by retaining only a

specific number of principal components following PCA, and then reconstructing the data set. Through careful selection of the number of principal components retained the residuals should ideally contain only noise and no chemical information, therefore removing noise from the data set. Good improvements in SNR were observed using the noise reduction algorithm when retaining the first 20 principal components. Since the samples had been de-waxed prior to imaging, considerable resonant Mie scattering (RMieS) could be observed in the recorded spectra.<sup>13</sup> The RMieS-ESMC pre-processing algorithm was utilised with 20 iterations on each of the data sets to correct for these scattering effects.<sup>20,21</sup> Spectra were then quality tested to remove areas of the images where no tissue was present. Quality testing was based on the intensity of the amide I band, with only spectra falling within an acceptance window of 0.07–2 being retained. Spectra were then truncated between 1700–2500 cm<sup>-1</sup> since this region contains little diagnostically relevant information. Furthermore the focus of this study is on the two ends of the spectrum, which exhibit the most obvious influence of the EFSW effect. Finally each spectrum was normalised to the intensity of the amide I band at 1655 cm<sup>-1</sup>.

## 3. Results and discussion

### 3.1. Chemical imaging

Fig. 1 shows photomicrographs revealing a 2.8 mm × 2.8 mm area of the tissues stained with H&E for the patients with BPH (1a–1c)i and prostate cancer (1d–1e)i. The chemical images obtained in transmission mode are shown for each of the five patients (Fig. 1(a–e)ii), rendered by calculating the ratio of absorption band intensity of 1080 : 1240 cm<sup>-1</sup>. This ratio was chosen because absorption bands at 1080 and 1240 cm<sup>-1</sup> have been shown by ourselves<sup>22</sup> and others<sup>2</sup> to highlight nuclei rich epithelial cells and protein rich areas respectively. An initial comparison of the chemical images obtained in transmission mode with the H&E micrograph reveals excellent qualitative agreement. Regions within the chemical image containing epithelium (bright yellow) and stroma (deep red) can be clearly discerned.

Differentiation of the various histological classes present in the tissue is facilitated by the high contrast present. For purposes of comparison the rendered images obtained in transfection mode from the ratio of the 1080 : 1240 cm<sup>-1</sup> bands are shown in Fig. 1(a–e)iii. In the absence of any optical confounding factors, the images in transfection should give very similar results to those obtained in transmission, the only difference being the better signal to noise ratio due to the double pass through the sample. Initial inspection of the chemical images obtained in transmission mode with transfection reveals that there are profound differences in the images obtained in the two sampling geometries. Fig. 1b(ii) and 1b(iii) show the chemical images for the second patient (BPH) in transmission and transfection mode respectively. The image obtained in transmission mode has several areas of glandular epithelium

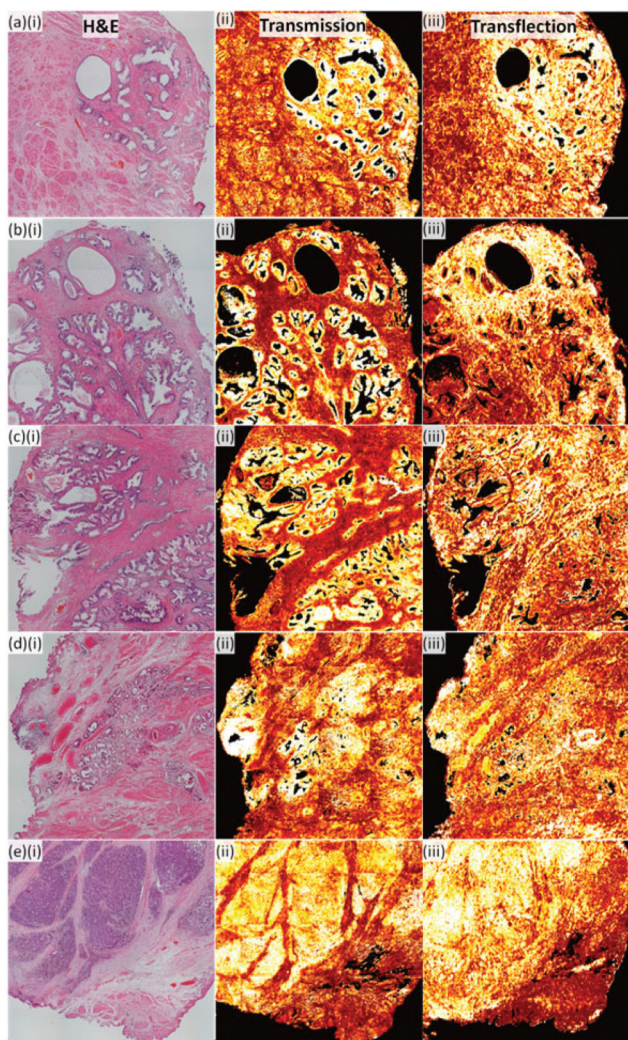


**Fig. 1** Imaging data for 5 patients (a–e) for the three contiguous serial sections respectively showing (i) H&E image, (ii) transmission chemical image of ratio  $1080 : 1240 \text{ cm}^{-1}$ , (iii) transflection chemical image of ratio  $1080 : 1240 \text{ cm}^{-1}$ .

(bright yellow) surrounded by the stoma (deep red), and the high contrast in the image allows these to be easily discerned. Areas identified as stroma from the H&E are rendered in the same colour in the chemical image and there is only limited false colour mixing within each histological class. Boundaries between the histological classes (for example epithelium and stroma) in the image are clear and distinct, enabling accurate segmentation of the classes. In transflection however, there is an obvious deterioration in the images acquired. The limited contrast within the image inhibits routine differentiation of the histological classes, and it is noticeable that areas of stroma have a large variability in the intensity of the rendered colouring in the image. These effects are due to spectral distortion occurring due to the so-called electric field standing wave effect which has been observed previously when utilising transflection slides for imaging biological materials.<sup>13,14,18</sup> The fact that this simple spectral biomarker is not transfer-

rable from one sampling modality to another poses a potential problem for the field of spectral pathology.

### 3.2. Spectral analysis

The chemical images displayed in the previous section demonstrate that hyperspectral images obtained in transmission and transflection are different and this is attributed to the electric field standing wave effect. This qualitative comparison although informative, does little to enhance our understanding of the magnitude of the spectral distortion effects at play. Quantitative analysis of the component infrared spectra is necessary for a meaningful comparison of chemical images obtained in each mode of operation. To achieve this, chemical images for each of the five patients were compared to the H&E stained sections to identify areas of epithelium. A database of epithelium spectra for each patient in both transmission and transflection was constructed using the methods previously reported by Fernandez *et al.*<sup>23</sup> A random sample of 1900 spectra from each database was extracted and the mean spectra obtained for each patient as shown in Fig. 2(a–e). The most striking observation in transmission mode of operation is that there is a high level of consistency in the mean spectra. Bands at  $3298 \text{ cm}^{-1}$  and  $1080 \text{ cm}^{-1}$  have intensity values which range from 0.46–0.50 and 0.13–0.16 respectively. This is to be expected considering that the spectra have all been normalised to the amide I band ( $1655 \text{ cm}^{-1}$ ) during spectral pre-processing. The transflection mean spectra exhibit significantly more variability, and this is particularly evident for the band at  $3298 \text{ cm}^{-1}$  whose intensity varies between 0.4–0.68 despite the pre-processing normalisation. The bands at  $1080 \text{ cm}^{-1}$  in the transflection mean spectra have intensities which range from 0.16–0.22. Other strategies for normalisation such as vector normalisation were also investigated and gave similar results showing that the non-linear spectral distortion across the spectrum is independent of normalisation.

Mean spectra provide useful information on the overall variability within a dataset, however more detailed information is provided through examination of absorption band strength for each spectrum in the database. The distributions of the band intensities at  $3298 \text{ cm}^{-1}$  and  $1080 \text{ cm}^{-1}$  are shown in histogram form in Fig. 3(a–e)i and 3(a–e)ii respectively. In transmission mode a Gaussian like distribution is observed for each of the bands and these have a narrow distribution indicating that for each patient the peak intensities fall within a narrow range. Furthermore the maximum of the distribution lies at or is very close to the same peak intensity for each of the five samples indicating that there is good reproducibility between patients.

Examination of the absorption band peak intensity distributions for the transflection data reveals significant differences when compared to transmission mode. An approximate Gaussian distribution is observed, however, there is a much wider distribution in band intensities. Variability in the position of the maximum of the distribution for each of the five patients is observed and there is less consistency suggesting that the normalised absorption band strengths for the epi-

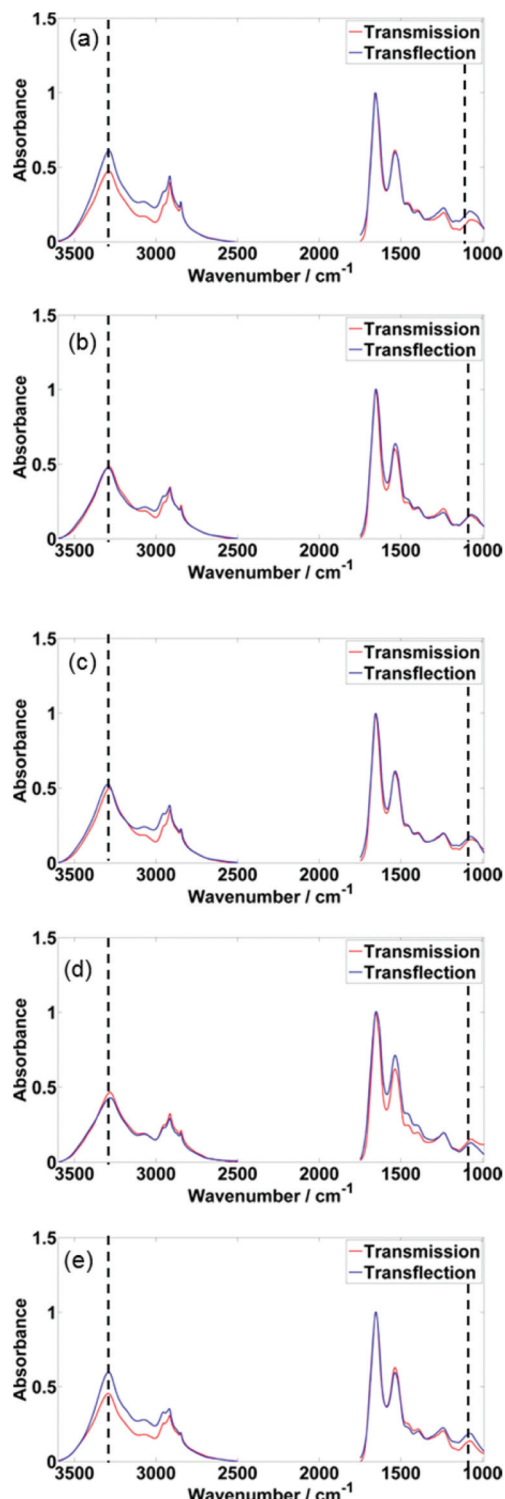


**Fig. 2** Mean spectra of transmission and transflection for each of the 5 patients. Dashed lines show the positions of the bands at  $3298\text{ cm}^{-1}$  and  $1080\text{ cm}^{-1}$ .

thelium spectra varies between patients when measured in transflection. The origin of the increased variability of absorption band intensity in transflection mode is inherently linked to the so-called electric field standing wave effect. In transflec-

tion mode, for a sample of uniform thickness, absorption bands at a given wavelength are expected to have similar intensities despite the EFSW effect. However, although the standing wave formed at the surface is expected to be reproducible provided the incidence angle is fixed, it is highly likely that there are variations in the thickness of the tissue on the transflection slide. Despite the use of robust sampling methodologies, rippling, smearing and drying artefacts often appear during the fixation process. Even tissue that is flat when cut (since the wax evens out any surface morphology) will become non-uniform when dewaxed. This is especially true for glandular tissue such as prostate which is full of "holes" and so by definition has inherent variability in tissue thickness. Distortions to the tissue are further exacerbated due to shrinkage occurring during the dewaxing and drying process. Given that the absorption band intensity depends on the integral of the square of a sinusoidal over the depth of the sample, small variations in thickness will have a profound effect on absorption band intensity. These distortions arising from the EFSW effect are the cause of the increased variability of absorption band intensity when operating in transflection mode.

We have also considered that the increased variability could simply be due to variations in heterogeneity between serial sections. The ability to investigate variability in absorption band intensity in the absence of heterogeneous effects, requires the same piece of tissue to be measured in each mode of operation. Unfortunately transflection and transmission measurements require the use of two optically different substrates, one being highly infrared reflective and the other being highly transmissive. Therefore it is currently technically impossible to analyse the same piece of tissue under both sampling modalities. However, measuring two contiguous serial sections under the same mode of operation would enable the variability due to heterogeneous effects to be studied.

Inter-section variability in transmission mode has been investigated using two,  $4\text{ }\mu\text{m}$  thick, serial sections of tissue mounted on a single  $\text{CaF}_2$  slide. The measurements were then repeated in transflection, on two further serial sections from the same patient fixed to a single MirrIR slide. A database of epithelium spectra was constructed from the data set and 1900 spectra randomly extracted. Fig. 4(i) shows histograms of the absorption band intensity distribution at  $3298\text{ cm}^{-1}$  in transmission mode for patient number 5 (CaP). In transmission mode a Gaussian like distribution is observed for each of the bands, and there is good overlap of band intensity between the two serial sections. The narrow distribution of absorption intensity is borne out through measurement of the width of the histograms. Serial section 1 and section 2 have a FWHM of 0.064 and 0.0451 at  $3298\text{ cm}^{-1}$ . Comparing the results obtained to those in transflection (Fig. 4ii) reveals clear differences between the two modes of operation. Gaussian like distributions are also observed but it becomes immediately obvious that the distributions are significantly broader. FWHM's for section 1 and 2 are 0.153 and 0.171 at  $3298\text{ cm}^{-1}$ . Therefore the transflection profiles for the bands  $3298\text{ cm}^{-1}$  are broader by a factor of approximately

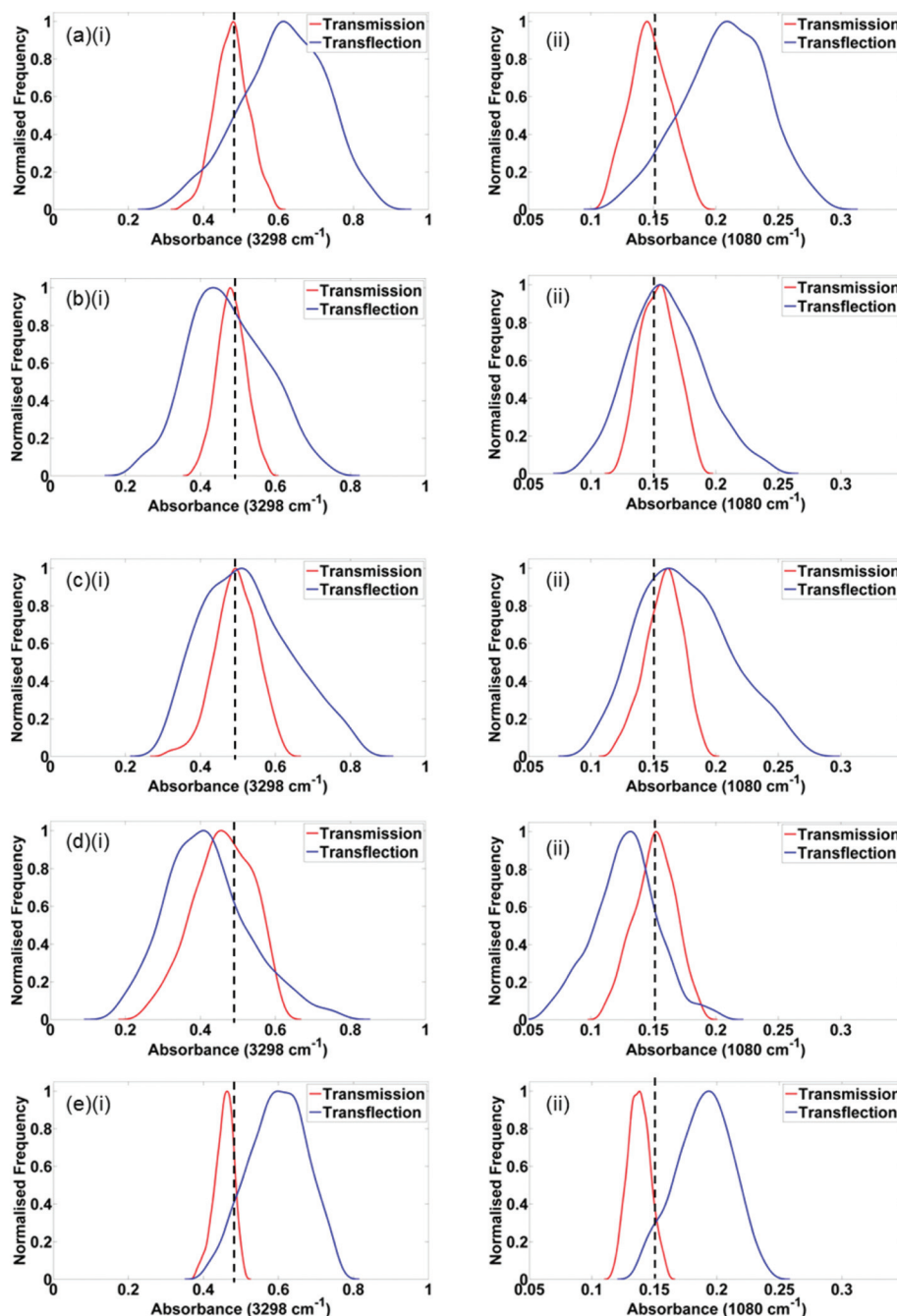


**Fig. 3** Distributions of absorbances obtained from 1900 epithelium spectra at (i)  $3298\text{ cm}^{-1}$  and (ii)  $1080\text{ cm}^{-1}$  for the 5 patients (a–e). The dashed vertical line represents the approximate midpoint of the peak intensity for both sampling modalities.

three when compared to transmission mode. Similar results are observed in Fig. 5(i), which shows the histograms of the absorption band intensity distribution at  $3298\text{ cm}^{-1}$  in transmission mode for patient number 2 (BPH). Gaussian profiles are again observed, and the lineshapes become significantly broader when in the transflection mode of operation.

Moreover, for both patients the histograms obtained from the serial sections for each sampling modality have an excellent degree of overlap and the lineshapes are almost identical.

Heterogeneity induced absorption band distribution broadening would be expected to be observed here as a change in peak width and lineshape for serial sections measured under the same mode of operation. The absence of these effects provides strong evidence that heterogeneous variations are not the cause of the variability which was observed in transflection. Therefore this demonstrates that changes to absorption band distributions in transflection are a direct consequence of mode of operation rather than heterogeneous variation between serial sections.

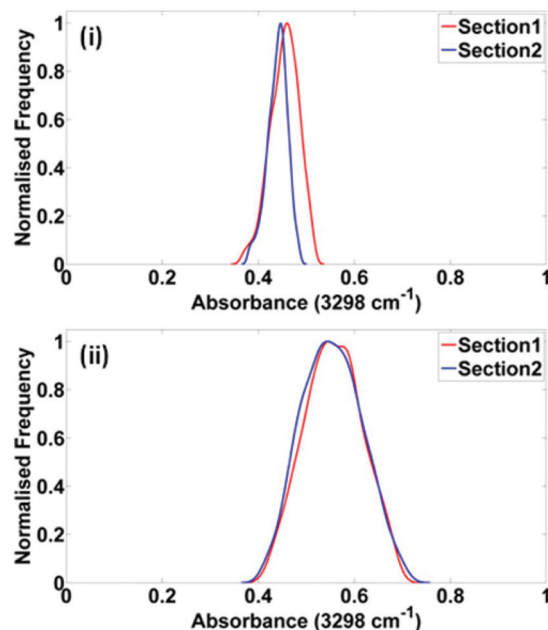


**Fig. 4** Distributions of absorbances obtained from 1900 epithelium spectra at  $3298\text{ cm}^{-1}$  for patient 5 (CaP) in modes of operation (i) transmission and (ii) transflection.

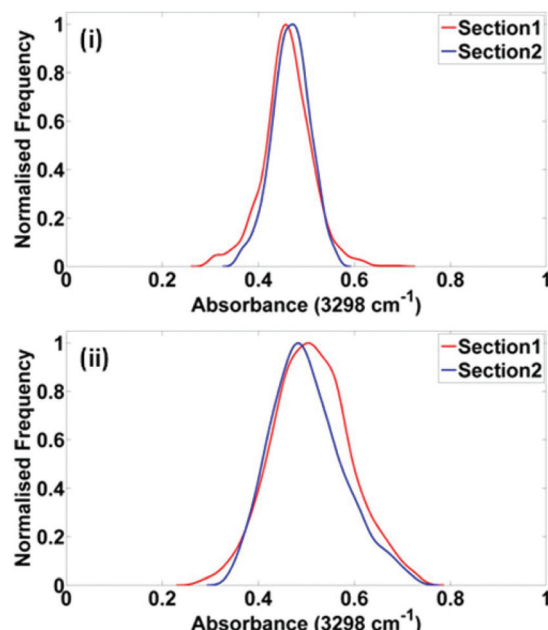


**Fig. 5** Distributions of absorbances obtained from 1900 epithelium spectra at  $3298\text{ cm}^{-1}$  for patient 2 (BPH) in modes of operation (i) transmission and (ii) transflection.

It is possible that the variability in absorption band intensity in transflection mode, is due to light passing through the sample twice,<sup>24</sup> thereby effectively doubling the path length through the tissue. We test this hypothesis by comparing the absorption band distribution in transmission mode, for serial

sections of prostate tissue of different thickness. If indeed the variability observed in transflection is due to the increased pathlength, then this effect should also be observed in transmission mode. Infrared images were obtained from two serial sections of prostate tissue, from a BPH patient, of  $4\text{ }\mu\text{m}$  and  $8\text{ }\mu\text{m}$  thickness mounted on calcium fluoride discs. The measurements were then repeated on two further serial sections ( $4\text{ }\mu\text{m}$  and  $8\text{ }\mu\text{m}$ ) from the same patient. Epithelium spectra were extracted from the IR chemical images obtained, and 850 spectra were selected at random from each of the four samples. Histograms of absorption band intensity distributions at  $3298\text{ cm}^{-1}$  for each of the four tissue sections are displayed in Fig. 6(i). Inspection of the histograms reveals almost identical distributions for each pair of samples (sample A and sample B), despite the different pathlengths through the tissue. The distributions are all Gaussian like and it is evident that the histograms are well centred on one another. Similar profiles are also observed in Fig. 6(ii) which shows the distribution of the absorption band intensity at  $1080\text{ cm}^{-1}$ .

Absorption band intensity variability can be quantitated through the mean FWHM for each pair of samples of the same thickness. The mean FWHM at  $3298\text{ cm}^{-1}$  for  $4\text{ }\mu\text{m}$  and  $8\text{ }\mu\text{m}$  samples are 0.142 and 0.127, and 0.0253 and 0.0267 at  $1080\text{ cm}^{-1}$  respectively. Therefore only minor differences in variability exist upon doubling the sample thickness. This strongly suggests that the variability observed in transflection is due to the sampling modality, and not due to the increased pathlength through the sample.

Variability between transmission and transflection sampling modalities is perhaps best illustrated through the use of PCA scores plots. Fig. 7 shows the PCA scores plot for patient 1 (BPH) for transmission and transflection. A tight cluster of the transmission data is observed, however the transflection data is much more diffuse and more broadly distributed. Furthermore the transmission and transflection data form two separate and distinct clusters, implying they have different chemical signatures. This is significant considering that both data sets arise from the same patient and from the same regions of epithelial cells, in adjacent tissue sections.

### 3.3. Diagnostics

Ultimately the feasibility of the utilisation of transflection infrared microscopy in clinical diagnosis will depend on the availability of models with high sensitivity and specificity. Crucially this will depend on how severe spectral distortions are, and what impact this has on classification of tissue as being malignant or benign. Machine based learning methods use training data to arrive at a series of metrics which can then be used to classify tissue as diseased or normal. Severe spectral distortions in the training data could ultimately limit the robustness of a model, potentially resulting in misdiagnosis with profound implications for the patient. It has been suggested that classifying tissue from a sample with different thickness to that used for the training data could result in misclassification and potentially misdiagnosis.<sup>14</sup> If the thickness of the tissue is the same, however, one might expect that this

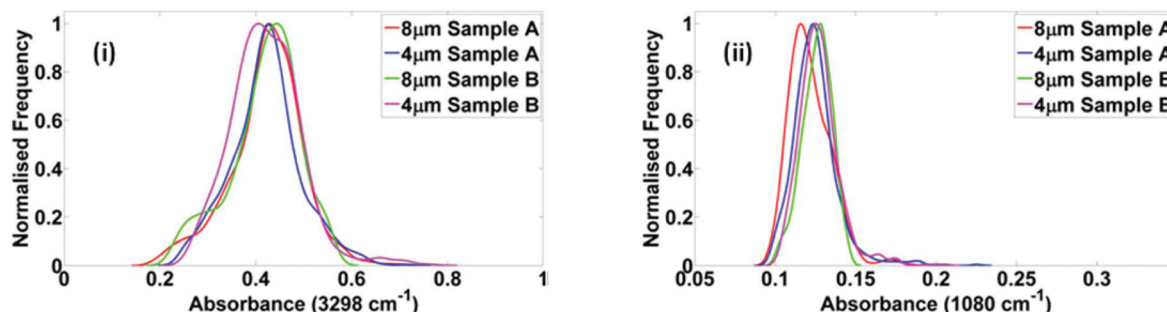


**Fig. 6** Distributions of absorbance band intensity obtained from 850 epithelium spectra for 4  $\mu\text{m}$  and 8  $\mu\text{m}$  sections at (i)  $3298 \text{ cm}^{-1}$  and (ii)  $1040 \text{ cm}^{-1}$ .

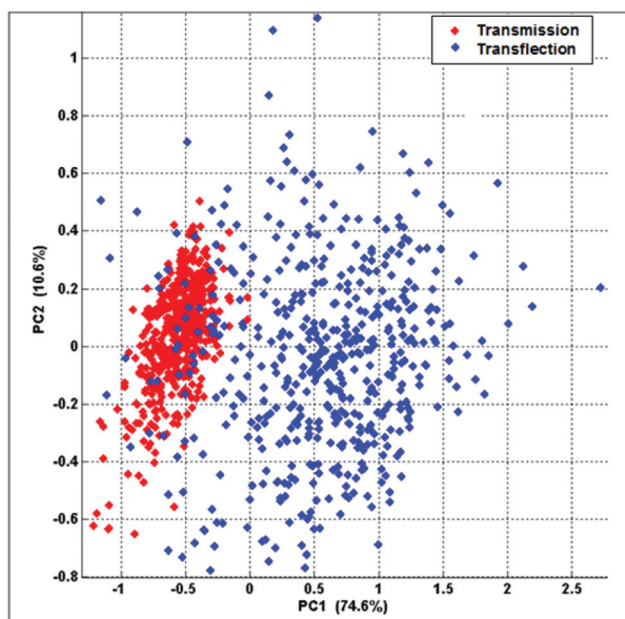


**Fig. 7** PCA scores plots for Patient 1 for transmission and transflection data.

in no longer a problem. We address this issue here by examining clustering for benign (BPH) and cancerous tissue (CaP) for the data set incorporating all five patients.

PCA scores plots are shown in Fig. 8a(i and ii) for transmission and transflection mode, for the spectra of epithelial tissue extracted from the database for all five patients. The plots show both PC1 and PC2, and the data points are coloured to identify if they originated from BPH (red) or CaP patients (blue), following review of the H&E by a trained pathologist. In transmission mode the clusters are relatively tight and although there is some intermixing there is clear separation between the clusters which enables discrimination between CaP and BPH. The clusters in transflection mode are significantly more diffuse, with considerable intermixing of data points making it difficult to identify any separation in the plot. Hanifi *et al.* attempted to reconcile transmission and transflection spectra through the use of the second derivative but found that significant differences remain.<sup>25</sup> In contrast

Cao *et al.*<sup>26</sup> demonstrated, in a limited study on dried cellular monolayers no difference was observed in classification between transmission and transflection when pre-processing the data set using a second derivative, which agreed broadly with an earlier study by Miljkovic *et al.*<sup>27</sup> We consider here the viability of using second derivative on our experimental data set to reduce the impact from the spectral distortion originating from the electric field standing wave effect.

The dataset was transformed to second derivative spectra using the Savitzky–Golay<sup>28</sup> method using a smoothing window of 7 data points. PCA scores plots for the derivatised data are shown in Fig. 8b(i and ii). Tight clustering is again observed in transmission mode and there is reasonable separation between the classes. Following second derivative there is some improvement in the separation of the clusters in the transflection PCA plot, however there is considerably more overlap compared to the transmission mode of operation.

## 4. Discussion

Numerous studies have now demonstrated that infrared analysis of clinical samples such as prostate cancer biopsy tissue sections can in principle be used to augment current histological practices and potentially aid diagnosis. The contrast in infrared hyper-spectral images is obtained directly from the heterogeneous chemical composition of the tissue. Rather than molecular biomarkers the technique relies on spectral biomarkers to discriminate tissue types and disease state. These spectral biomarkers represent a net change of a large number of different molecules representing the chemical constituents of the tissue. These spectral biomarkers are generally a combination of peak intensities and peak position of single or indeed multiple vibrational bands. In order for this new technology to be translated successfully into a clinical environment and be accepted as a routine pathology tool a number of conditions should be met. The barrier that we currently face is that two such issues, namely (i) low cost and robustness of substrate and (ii) reliability and robustness of spectral biomarkers, have conflicting solutions. There is no doubt that  $\text{CaF}_2$  or  $\text{BaF}_2$  slides generally used for transmission are expensive in comparison with low emissivity reflecting substrates.

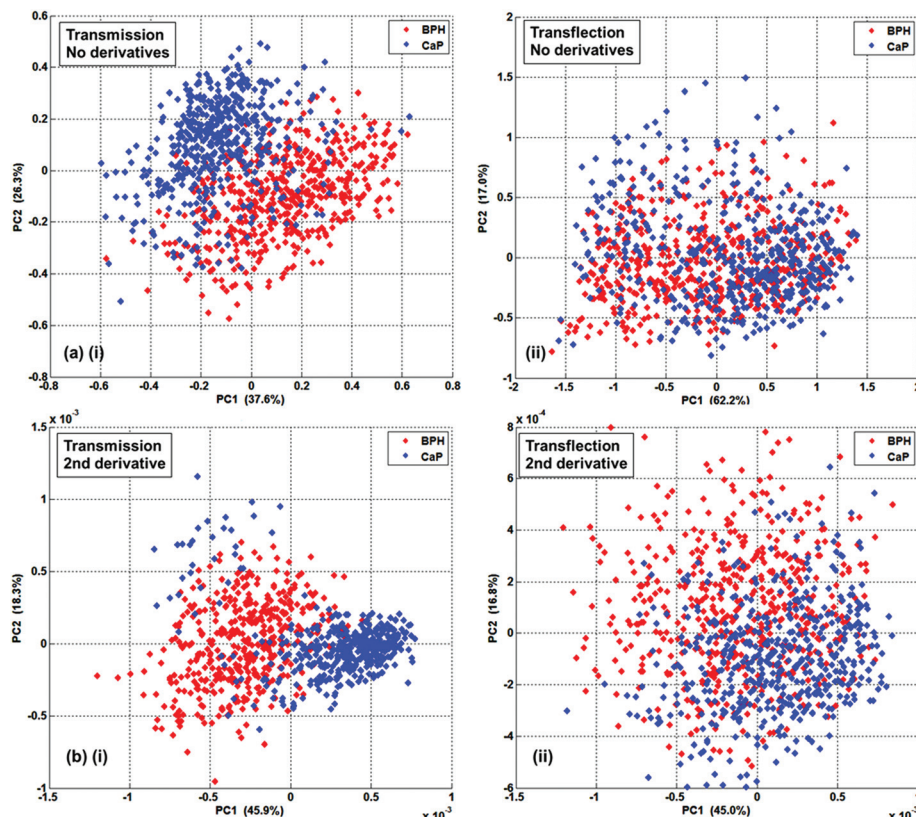


**Fig. 8** (a)(i) PCA result for transmission data for BPH and CaP for all the patients in no derivative mode. (b)(i) PCA for transmission but using second derivative. (a)(ii) The transflection data, no derivatives, (ii) second derivative.

The factor of 40 or so difference in price is substantial given the number of biopsy samples that are evaluated every year would wide. It could be argued that the price of transmission substrates would reduce with wide spread use but whether the gap between these substrates and the cheaper low-e microscope slides would still be a significant barrier to adoption is unclear. It is also the case that  $\text{CaF}_2$  or  $\text{BaF}_2$  slides have other inherent disadvantages. The most obvious one is that they are brittle and fragile. This is a serious obstacle to widespread adoption since it would require significant deviation from the usual work flow and standard operating protocols used in clinical practice.  $\text{CaF}_2$  or  $\text{BaF}_2$  slides will not go through current automated systems used for tissue preparation since the chances of them fracturing and disrupting the whole process is simply too high. Other more robust polymer substrates might be applicable but these are yet to be fully evaluated. Glass is a potential alternative although necessitates working with an extremely restricted spectral range.<sup>29</sup>

Despite the problems with  $\text{CaF}_2$  or  $\text{BaF}_2$  slides this paper demonstrates, quite clearly, that tissue analysis on the cheaper low-e slides is not without significant problems. The non-linear optical distortion means that essentially identical tissue sections measured using different sampling modalities give different spectra. The result of this is that a simple spectral bio-marker (in this case the  $1080:1240\text{ cm}^{-1}$  ratio) is not transferable from one measurement system to another. More

importantly, while the spectral biomarkers are independent of sample thickness in transmission they are dependent on thickness in transflection. This is potentially a problem when “selling” the technique to either end users or indeed potential investors. It can be demonstrated that under controlled conditions this issue can be negated by having very precise control over sample preparation and in particular the accuracy of the slicing of the tissue sections and indeed this has been done to very good effect by Kochan *et al.* in this special issue.<sup>24</sup> A classification model build on a data base of spectra will be transferrable to unknown tissue sections provided they have been cut at exactly the same thickness. Variations in thickness, however, will undoubtedly reduce the robustness of the classification model. These variations may come due to the generally accepted error in the accuracy of a microtome (estimated to be between 4 and 7% with a rotary microtome) but also in human operator error.<sup>30</sup> This can be eliminated in a controlled study as evidence but is likely to be a much more significant factor if samples are being obtained from many different hospital labs where operators have been trained very differently and may have very different work practices. In addition, even if the cut sample is of the correct thickness when it leaves the microtome there is significant distortion mainly due to shrinkage resulting from the dewaxing and drying process.<sup>31,32</sup> Uneven shrinkage in the  $z$  direction is the most likely origin of much of the heterogeneity in the transflection spectra. This

could be avoided in part by using non dewaxed tissue<sup>22,33</sup> but this means sacrificing the lipid region of the spectrum and at present this is not common practice.

## 5. Conclusions

- In this paper we show that spectra from serial tissue sections measured using transfection mode exhibit a significant increase in variation of absorbance across the spectrum, compared with equivalent spectra measure in transmission. This variation has been attributed to non-linear distortions in absorption band intensity arising from the EFSW effect.

- Data from essentially the same tissue and of the same region of epithelial cells were shown to exhibit significant differences when measured in transmission and transfection mode.

- Serial sections measured with the same sampling modality exhibit no significant differences in absorption band intensity variability, proving spectral distortions observed in transfection are not due to the heterogeneous nature of serial sections.

- Doubling the sample thickness in transmission resulted in no significant differences, indicating that the increased pathlength in transfection is not responsible for the increased absorption band variability.

- The spectral biomarkers in this study were not transferable from one measurement mode to another.

- The use of second derivatives partially alleviates the problems caused by the distortion in the case of prostate tissue.

- In general, the extent to which the biological difference can be recovered will depend upon the relative strength of these differences compared with the distortion. In the case of a very obvious biomarker we would expect that the classification can be made using either transmission or transfection mode. In the case of much more subtle differences, it is likely that these will be obscured in transfection mode but not in transmission. In transmission mode the limiting factor will be the signal to noise ratio.

- In exploratory analysis where spectral differences are not known before hand, true differences may be masked by the transfection mode distortion. We suggest that exploratory studies be done in transmission mode and when appropriate spectral biomarkers are found, the application is re-produced in transfection mode to validate the spectral markers are still present. Under such circumstance meaning that low-e slides could still be a viable substrate for some clinical applications.

## Acknowledgements

We would like to thank EPSRC for funding (Grant reference EP/K02311X/1). We would like to thank Mick Brown for obtaining additional tissue for us at short notice.

## Notes and references

- H. H. Mantsch, *Analyst*, 2013, **138**, 3863–3870.
- R. Bhargava, *Anal. Bioanal. Chem.*, 2007, **389**, 1155–1169.
- B. Bird, M. J. Romeo, M. Diem, K. Bedrossian, N. Laver and S. Naber, *Vib. Spectrosc.*, 2008, **48**, 101–106.
- C. Kendall, M. Isabelle, F. Bazant-Hegemark, J. Hutchings, L. Orr, J. Babrah, R. Baker and N. Stone, *Analyst*, 2009, **134**, 1029–1045.
- J. B. Lattouf and F. Saad, *BJU Int.*, 2002, **90**, 694–698; discussion 698–699.
- M. J. Baker, E. Gazi, M. D. Brown, J. H. Shanks, P. Gardner and N. W. Clarke, *Br. J. Cancer*, 2008, **99**, 1859–1866.
- E. Gazi, M. Baker, J. Dwyer, N. P. Lockyer, P. Gardner, J. H. Shanks, R. S. Reeve, C. A. Hart, N. W. Clarke and M. D. Brown, *Eur. Urol.*, 2006, **50**, 750–761.
- E. Gazi, J. Dwyer, P. Gardner, A. Ghanbari-Siahkali, A. P. Wade, J. Miyan, N. P. Lockyer, J. C. Vickerman, N. W. Clarke, J. H. Shanks, L. J. Scott, C. A. Hart and M. Brown, *J. Pathol.*, 2003, **201**, 99–108.
- E. Gazi, J. Dwyer, N. P. Lockyer, J. Miyan, P. Gardner, C. A. Hart, M. D. Brown and N. W. Clarke, *Vib. Spectrosc.*, 2005, **38**, 193–201.
- K. M. Gough, L. Tzadu, M. Z. Kastyak, A. C. Kuzyk and R. L. Julian, *Vib. Spectrosc.*, 2010, **53**, 71–76.
- E. Gazi, J. Dwyer, N. Lockyer, P. Gardner, J. C. Vickerman, J. Miyan, C. A. Hart, M. Brown, J. H. Shanks and N. Clarke, *Faraday Discuss.*, 2004, **126**, 41–59.
- K. R. Flower, I. Khalifa, P. Bassan, D. Demoulin, E. Jackson, N. P. Lockyer, A. T. McGown, P. Miles, L. Vaccari and P. Gardner, *Analyst*, 2011, **136**, 498–507.
- P. Bassan, J. Lee, A. Sachdeva, J. Pissardini, K. M. Dorling, J. S. Fletcher, A. Henderson and P. Gardner, *Analyst*, 2013, **138**, 144–157.
- J. Filik, M. D. Frogley, J. K. Pijanka, K. Wehbe and G. Cinque, *Analyst*, 2012, **137**, 853–861.
- B. J. Davis, P. S. Carney and R. Bhargava, *Anal. Chem.*, 2010, **82**, 3474–3486.
- B. J. Davis, P. S. Carney and R. Bhargava, *Anal. Chem.*, 2010, **82**, 3487–3499.
- R. G. Greenler, *J. Chem. Phys.*, 1966, **44**, 310–315.
- H. Brooke, B. V. Bronk, J. N. McCutcheon, S. L. Morgan and M. L. Myrick, *Appl. Spectrosc.*, 2009, **63**, 1293–1302.
- C. Hughes, L. Gaunt, M. Brown, N. W. Clarke and P. Gardner, *Anal. Methods*, 2014, **6**, 1028–1035.
- P. Bassan, A. Kohler, H. Martens, J. Lee, H. J. Byrne, P. Dumas, E. Gazi, M. Brown, N. Clarke and P. Gardner, *Analyst*, 2010, **135**, 268–277.
- P. Bassan, A. Kohler, H. Martens, J. Lee, E. Jackson, N. Lockyer, P. Dumas, M. Brown, N. Clarke and P. Gardner, *J. Biophotonics*, 2010, **3**, 609–620.
- P. Bassan, A. Sachdeva, J. H. Shanks, M. D. Brown, N. W. Clarke and P. Gardner, *Proc. SPIE-Int. Soc. Opt. Eng.*, 2014, 9041.
- D. C. Fernandez, R. Bhargava, S. M. Hewitt and I. W. Levin, *Nat. Biotechnol.*, 2005, **23**, 469–474.

- 24 K. Kochan, P. Heraud, M. Kiupel, V. Yuzbasiyan-Gurkan, D. McNaughton, M. Baranska and B. R. Wood, *Analyst*, 2015, DOI: 10.1039/c4an01901f.
- 25 A. Hanifi, C. McGoverin, Y. T. Ou, F. Safadi, R. G. Spencer and N. Pleshko, *Anal. Chim. Acta*, 2013, **779**, 41–49.
- 26 J. Cao, E. S. Ng, D. McNaughton, E. G. Stanley, A. G. Elefantiy, M. J. Tobin and P. Heraud, *Analyst*, 2013, **138**, 4147–4160.
- 27 M. Miljkovic, B. Bird, K. Lenau, A. I. Mazur and M. Diem, *Analyst*, 2013, **138**, 3975–3982.
- 28 A. Savitzky and M. J. E. Golay, *Anal. Chem.*, 1964, **36**, 1627–1639.
- 29 P. Bassan, J. Mellor, J. Shapiro, K. J. Williams, M. P. Lisanti and P. Gardner, *Anal. Chem.*, 2014, **86**, 1648–1653.
- 30 A. Anthony, G. J. Colurso, T. M. A. Bocan and J. A. Doebler, *Histochem. J.*, 1984, **16**, 61–70.
- 31 A. Smith, *Stain Technol.*, 1962, **37**, 339–345.
- 32 A. D. Pearse and R. Marks, *J. Clin. Pathol.*, 1974, **27**, 615–618.
- 33 P. Bassan, A. Sachdeva, J. H. Shanks, M. D. Brown, N. W. Clarke and P. Gardner, *Analyst*, 2013, **138**, 7066–7069.